Article

Photonic Properties of Colloidal Crystal Elastic Sheets Formed by Electrostatic Repulsion and Shear Stress and Their Fundamental Deformation Modes

Hiroshi Fudouzi [1,*], Tsutomu Sawada [1], Satoshi Kawanaka [2], and Fumio Uchida [2]

[1] National Institute for Materials Science, 1-2-1, Sengen, Tsukuba 305-0047, Japan
[2] Fuji Chemical Co., Ltd., 1-35-1, Deyashikinishi-machi, Hirakata-shi 573-0003, Japan
* Correspondence: fudouzi.hiroshi@nims.go.jp
Received: 3 March 2025; Revised: 21 April 2025; Accepted: 23 April 2025; Published: 15 May 2025

Abstract: Recently, mechanochromic soft materials that enable smart sensing functions by visual inspection without the need for special devices have been attracting attention. We have developed a non-close-packed type elastic colloidal crystal sheet through a simple shear-induced process. The colloidal crystal state, in which the (111) plane exhibited significant orientation due to shear stress, was successfully stabilized in the 4-hydroxybutyl acrylate (4-HBA) monomer precursor dispersed with desalted silica colloidal particles through the implementation of UV irradiation radical polymerization. Consequently, a solid colloidal crystal sheet was produced, capable of reversibly modulating its structural color in response to elastic deformation. In this article report will address the stress response functions of this sheet due to elastic deformation of stretching, compressing and bending. In addition, a rapid structural color change at 4.17 ms unit by impacting. By analysis of tensile and strain curve, Young's module was 0.56 MPa, tensile strength 0.73 MPa and elongation brake was 142.9%. In addition, durability repeating elongating the rubber sheet for 100,000 times. Up now 150 cm^2 sheet produced by hand made batch process. This simple process is suitable for scaling up colloidal crystal to mass production and is expected to have a wide range of engineering applications with mechanochromic materials.

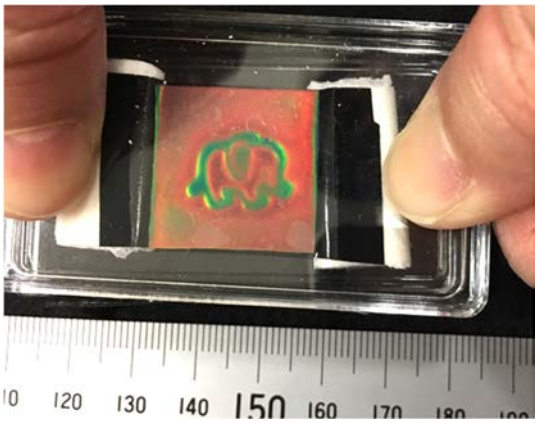

Keywords: silica colloids; poly (4-hydroxybutyl acrylate) elastomer; non-close-packed colloidal crystal; shear stress; elastic deformation; Bragg's diffraction; structural color

1. Introduction

In recent years, the study of mechanochromism, in which the structural color of soft materials changes because of deformation or stress, has become increasingly popular [1–3]. Multilayer films [4], block copolymers [5,6], liquid crystal elastomers [7], and colloidal crystals [8], including opal [9], inverse opal types [10] and core-shelll colloidal powders [11], have been studied and attempted to be applied to smart materials in a wide range of fields, from sports, medical, smart skin, and infrastructure damage detection. For engineering applications, a Role-to-Role coating process, which has been applied to hydroxypropyl cellulose [12] and core-shell colloids [13], has made mass production possible.

Elastic non-close-packed type colloidal crystal is one of important soft materials to produce smart materials with tuning structural color by mechanical deformation. There are two approaches; Core-shell nanospheres were applied thermally shear stress [11,13] and polymerization repulsively charged colloidal crystals embedded in monomer and polymerization. The later approach is traditional approach to form non-close packed colloidal crystal in hydrogel [14]. This method allows colloidal particles to be dispersed in a monomer liquid that does not contain a water-soluble solvent instead of a hydrogel. Recently, non-close packed type of elastic colloidal crystals has been attracting much attention due to their wide range of structural color tuning and rubber-like mechanical

properties. Methods have been reported in which silica particles are dispersed in an acrylic monomer that does not contain aqueous solvent and then polymerized into an elastomer by radical reaction [15–18], and another method in which a high-quality colloidal crystal embedded in hydrogel is formed and then replaced with an acrylic monomer to form an elastomer [19]. Research in this field is expected to have applications in smart skins and other areas and has been actively pursued in recent years. For example, research is progressing on the analysis of the relationship between changes in the microstructure (crystal lattice) of colloidal crystals due to deformation and their optical properties [20]. Additionally, a new type of elastomer that does not change structural color under elastic deformation has been reported [21]. Furthermore, studies are underway to enhance functionality by combining mechanochromic properties with other functionalities, such as electronic-optical [22] and magnetic-optical [23] responses.

Sawada et al., have been investigating colloidal photonic crystals made of soft materials: hydro gels and elastomers [24]. In the previous works, deionized colloidal particles suspension easily form colloidal crystals and furthermore the quality of colloidal crystal improved by adjusted applied shear flow. However, colloidal crystal embedded in hydrogel sheet is too soft and wetted with solvent. From a viewpoint of applications like rubber, solvent free is better. Thus, silica colloids were dispersed in monomer and deionized by ion exchange resin. Deionization causes colloidal particles to form crystals, resulting in a reflection peak. It is believed that removing residual Na^+ ions and other impurities from silica particles during synthesis causes the electric double layer around colloidal particles to expand, leading to electrostatic repulsion and an Alder phase transition, thereby forming colloidal crystal. Highly charged silica formed a repulsion layer and formed multi-crystals colloidal crystal in monomer liquid. It is well known that shear stress is important for forming orientated colloidal crystal [25]. A shear stress method was used as following procedure and finally monomer liquid was changed to solid rubber like elastomer by polymerization of UV radical reaction [26]. Non close packed colloidal crystal with uniform structural color is important for practical mechanochromic applications.

Figure 1 shows the concept image of the process. (A) Preparing UV-curable colloidal dispersion: silica nanosphere are dispersed in UV-curable acrylate monomer liquid, (B) Randomly oriented colloidal crystal grins are formed by deionization originated from electrostatic repulsion layer expanding, (C) Orientation of colloidal crystal planes due to shear stress near the glass plate, and (D) UV-radical polymerization of liquid monomer to solid without broking colloidal crystal, as a result non-close-packed type silica colloidal crystal to fix in solid elastomer. As described later, deionized treatment improves the uniformity of structural color for large size (over 150 cm^2) in colloidal crystal embedded in elastomer sheet. The objective of this study is to provide a comprehensive report on the fundamental photonic functions of an elastic colloidal crystal sheet under typical deformation modes, including stretching, compression, and bending. Furthermore, we have demonstrated a simple and pragmatic photonic functions of elastic colloidal crystal rubber, including strain imaging through the impact of an object and the durability of a large number of cyclic deformations.

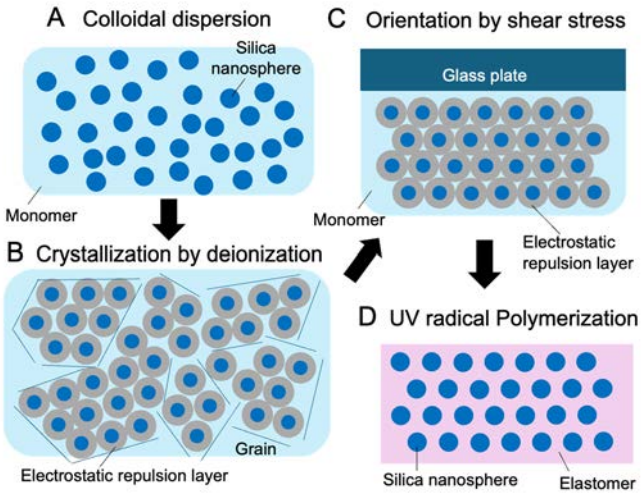

Figure 1. Conceptual diagram of the process for producing colloidal crystal highly-oriented in an elastomer matrix using electrostatic repulsion. (**A**) silica nanospheres are well dispersed in a precursor liquid of monomer, (**B**) ion exchange resin is used to deionize the colloids to form small size grains of colloidal crystal with random orientation planes, (**C**) the colloidal crystals are oriented in one direction by shear stress near the glass plate, and (**D**) the precursor is polymerized by UV irradiation with a radical initiator, and the colloidal crystals are immobilized in the elastomer.

2. Materials and Methods

As a precursor, silica nanospheres were dispersed in UV curable monomer liquid. Monodispersed silica nanosphere (Silbol 150, Fuji Chemical Co., Ltd., Osaka, Japan) was dispersed in 4-Hydroxybutyl Acrylate (4-HBA, Osaka Organic Chemical Industry Ltd., Osaka, Japan). 2-Hydroxy-2-methylpropiophenone (Sigma-Aldrich, St. Louis, MO, USA) is a radical photo-initiator (PI) molecule that was used in the polymerizing 4-HBA monomer by exposure of UV radiation. AG 501-X8 Mixed Bed Resin, biotechnology grade (Bio-Rad Laboratories, Inc., Hercules, CA, USA) was selected as deionized ions from the precursor monomer of 4-HBA and silica colloids.

The concentration of silica in the dispersion was 20 wt% was mixed with 1 wt% PI by tube rotator for 30 min. The de-ionized dispersion indicates a milky bright structural color due to Bragg's diffraction from small grain sized colloidal crystals. Supplemental Figure S1 shows a conceptual flow of making rubber sheet from deionized 4-HBA precursor. This deionized 4-HBA precursor silica suspension was infilled into a between two glass substrates with a 1 mm spaced gap for applying shear stress, as shown in Figure S1B. The lower glass substrate by uniaxial vibration indued a shear stress to 4-HBA precursor. The typical vibration motion was 10 Hz and amplitude length of 1 mm (Vibration shaker (SSV-105) and controller (SVA-ST-30), San-Esu Co. ltd., Tokyo, Japan). As a result, the structural color became more vivid as many small colloidal crystal grains with randomly oriented planes were oriented perpendicular to the glass surface. After stopping the vibration, UV LED light was irradiated through the glass plate as shown in Figure S1C. The 4-HBA liquid changed solid elastomer.

A 365 nm UV LED array (MBRL-CUV7530, 4.3 W LED module and MLEK-A230W2LRDB controller, MORITEX Co., Yokohama, Japan) was used for UV irradiation. As a result, 4-HBA monomer was polymerized to homopolymer with highly (111) plane-oriented colloidal crystal. The glass transition temperature of poly(4-HBA) elastomer is—40 degrees C and shows elastic function like rubber. The LED modules (75 mm × 30 mm) were joined and cover the entire area of the standard sample size, 100 mm × 100 mm. After UV curing, poly (4-HBA) elastomer sheet with uniform structural color was obtained, and a free-standing elastomer sheet of 1 mm thickness was formed by peeling from glass sheet. To support the mechanical strength and improve the structural color, the elastic poly(4-HBA) sheet was bonded to a 1 mm thick black colored chloroprene rubber CR sheet (CB260N, 1 mm thickness, AKITSU Industry Co., Ltd., Hiroshima, Japan).

3. Measurement and Equipment

The reflectance spectra of the poly (4-HBA) elastomer sheets and silica colloid dispersions of monomer were recorded using a miniature fiber optic spectrometer (Ocean Optics, USB2000+, Dunedin, FL, USA). The incident light was perpendicular to the samples (to measure specular reflectance, the probe was oriented at 90° to the sample in a reflectance probe holder) at a local spot (less than 2 mm in diameter) by HL-2000 tungsten halogen light source. The fiber has a core diameter of 200 μm, a numerical aperture of 0.22, and is banded with six illumination fibers around a single read fiber. Using this probe fiber, we measured the reflectance to analyze the shift of the Bragg diffraction peaks due to elastic deformations. In addition, transmittance spectroscopy at different angles of incidence was used to estimate the spacing of the silica array planes. A UV/VIS spectrophotometer with a variable angle specular transmittance accessory (V-570, JASCO Co., Tokyo, Japan) was used. This simple analysis method was reported in our previous paper [27]. In the transmission spectrum, the wavelength position of the valley corresponds to the wavelength of the Bragg diffraction peak. By analyzing the correlation between the angle of incidence and the wavelength of the valley, the interplanar spacing of the particle array plane can be determined. Refractive index of monomer 4-HBA and poly(4-HBA) elastomer was measured with an abbe refractometer at the wavelength of D-Line (NAR-1T SOLID, ATAGO Co., Ltd., Tokyo, Japan).

Reflection photo image and movie were obtained under using a flat high brightness LED white light (LED viewer 5000A, Color temperature: 5000 K, Shinkosha, Co., Tokyo, Japan) irradiation. Digital camera (EXILIM EX-F1, CASIO Computer Co., Ltd., Tokyo, Japan) and with a smart phone camera with 240 fps slow movie mode (iPhone 6 Plus, Apple Inc., Cupertino, CA, US). A part of photo images was taken using a coaxial vertical illumination to obtain uniform structural color image. Stretching and bending of rubber sheets was done by a one-axis manual stage. Compression and impact experiments were conducted using a homemade device shown in the attached figures below.

Stress-strain curves were measured by uniaxial tensile equipment (ZTA-500N+FSA-1KE-500N, IMADA Co., Ltd., Aichi, Japan). The Danbel-shaped test piece with 1.03 mm thickness was punched out using a metal template (JIS K6251 #8). The width of center was 4 mm. Initial length of the test piece was 28 mm between gripping's length. Due to technical reason, the elongation of test piece was measured as the gripping's length. Durability test was performed by desktop model endurance test machine (DMLHP-PP, Yuasa System Co., Ltd.,

Okayama, Japan). The elastomer had a width of 10 mm, an initial length of 40 mm, and an elongated length of 55 mm. The elongation was 55/40 = 137.5%.

4. Results & Discussion

4.1. Deionized Silica Colloidal Crystal in 4-HBA Monomer Liquid

Figure 2 shows the analysis of the Bragg's diffraction of the silica colloidal crystals dispersed in monomer liquid formed by deionization. Figure 2A shows typical reflection spectrum with and without deionization treatment. Silica of 150 nm diameter colloids were dispersed in 4-HBA monomer liquid and deionization using ion-exchange resin. A single diffraction peak appears around 653 nm after deionization. This single peak due to Bragg's diffraction from array of silica colloidal crystal planes. Supplemental Figure S2 compares two cuvettes at 20 wt% silica colloids, the left with de-ionization shows light red color and the right without deionization as shown in the photo A. The left cuvette shows light red color due to the Bragg's diffraction of 653 nm peak. The color of the cuvette is strongly influenced by the direction of the incident light. In the photo C, the light is reflected specularly, and the color appears red. In the photo D, the light is reflected at a 90° angle and the color appears light green or light blue. In the photo B, the light is reflected at a 45° angle and the color of the fiber illumination appears light orange, while the color of the light reflected at a 90° angle appears light green. From these observations, we can conclude that the color is a structural color with angle dependence.

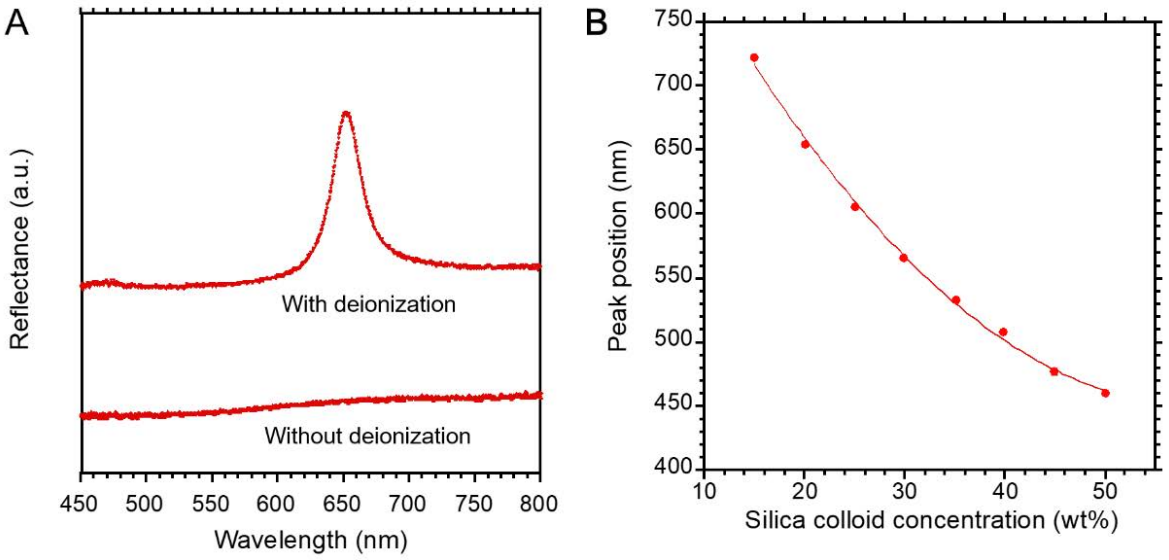

Figure 2. Colloidal crystals formed by silica colloidal particles dispersed in monomer (4-hydroxybutyl acrylate, 4HBA) liquid. (**A**) The effect of deionization treatment using ion exchange resin on crystallization, (**B**) The effect of silica particle concentration on the reflection peak wavelength of the colloidal crystal.

Supplemental Figure S3 shows the silica concentration effect changes the structural color of colloidal crystal in 4-HBA monomer liquid. At low concentration of 15 wt% shows red and high concentration of 50 wt% shows purple. This color change depends on peak shift of the diffraction peak at specular reflection. The diffraction peak position corresponds to the silica particle concentration as shown in Figure 2B. The peak position wide varied from 460 nm to 722 nm, i.e., covering from almost entire visible color region to near NIR region. This means that the lattice distance of colloidal crystal can be tuned by only particle concentration silica colloids in wide visible color range [13,14]. In this paper, we selected initial structural color as red for colloidal crystal rubber sheet for tunable structural color function by mechanical deformations for wide color changeable range.

4.2. Silica Colloidal Crystal in Poly(4-HBA) Elastomer Solid Sheets

Figure 3 shows the uniaxial tensile stress-strain curves of silica colloidal crystals in a poly(4-HBA) elastomer sheet. Photo A shows the elongation of the elastomer sample just before fracture. At the time of fracture, the tensile stress was 3.0 N, and the elongation was 40 mm, as shown in Figure 3B. The tensile strength was calculated to be 0.728 MPa. The elongation at break was 142.9%. The Young's modulus (elastic modulus) can be determined from the slope of the strain-stress curve. Therefore, the Young's modulus was derived from the slope under the low-

load conditions (less than 35%) shown in Figure 3C. The correlation coefficient exceeded 0.998, and the Young's modulus was 0.56 MPa.

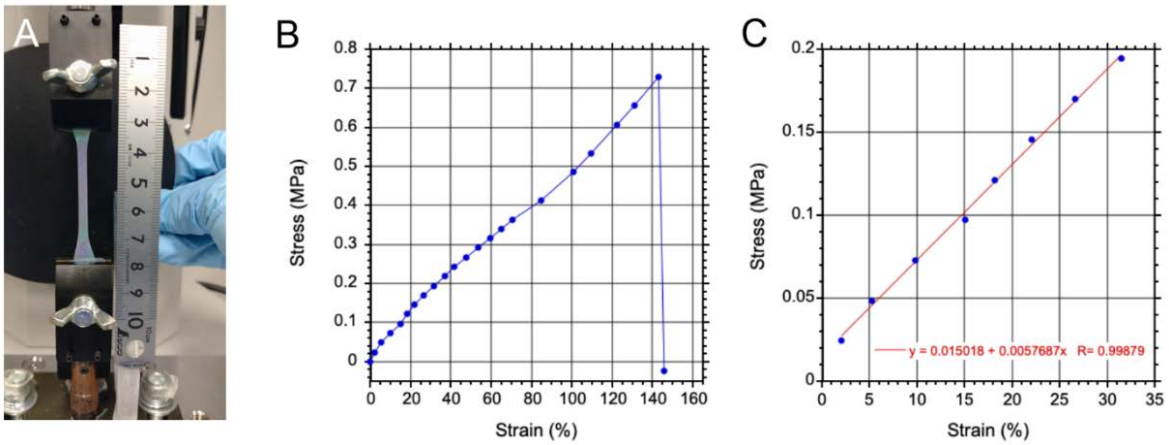

Figure 3. Mechanical property measurement by uniaxial tensile. (**A**) Stretched danbel form specimens, (**B**) Stress-strain curves were plotted up to the point of failure and (**C**) Stress-strain curves at low load conditions.

Figure 4 shows silica colloidal crystals embedded in 4-HBA on a black color supporting CR rubber sheet. Figure 4A shows a uniform structural color over an area of almost 100 mm × 100 mm. The structural color of 4-HBA elastomer is brighter red, peak position around 637 nm. The refractive index of monomer 4-HBA was 1.452, and that of 4-HBA elastomer was 1.493 at 25 °C. On the other hand, the refractive index of the silica colloid is about 1.45, and the refractive index contrast increases as polymerization progresses from monomer to elastomer. This may be one of the reasons why UV radical polymerization contributes to the vividness of the structural color. The photo image was taken using a coaxial vertical illumination. Figure 4B shows a conceptual diagram of the cross-section of the rubber sheet. Colloidal crystal layer was 1 mm and thickness of the black color rubber sheet is also 1 mm. The white light incident at right angles to the colloidal crystal is split into reflected and transmitted light at the alignment planes of the silica particles. The reflected light, due to Bragg's diffraction, depends on the spacing between the alignment planes and causes the red structural color in Figure 4A. Light of other wavelengths transmitted through the colloidal crystal is absorbed by the black supporting rubber sheet. The Bragg's diffraction peak can be expressed by as following equation [27].

$$\lambda = 2d \sqrt{\left(n_p^2 V_p + n_m^2 V_m\right) - \sin^2 \theta} \quad (1)$$

Here, λ is the peak position, d is the interspacing between the particle array planes, n_p is the refractive index of the colloidal particles, V_p is the volume of the colloidal particles, n_m is the refractive index of the matrix, V_m is the volume of the matrix, and θ is the angle of the incident light. Figure 5 shows the transmittance spectrum at different tilting angles θ and delivered the linear relationship derived from Equation (1). Here due to a simple measurement method, the Bragg's diffraction peaks were corresponding to the dips in the transmission spectrum. From the slope of the line in Figure 5B is 0.4775, the interspacing of silica planes, d was obtained as 229.5 nm. In the case of a colloidal crystal with silica particles arranged in the closest packing of 150 nm silica colloid, the distance between the planes of the silica array can be calculated to be 122.5 nm. Therefore, the difference in interplanar spacing between the non-closest packed and closest packed colloidal crystals is 107 nm, which is a maximum displacement that can change the interplanar spacing. This corresponds to a wavelength of approximately 289 nm when converted to the wavelength of the diffracted peak. The wavelength of the initial state of the non-close-packed colloidal crystal elastomer is 637 nm (red), and it covers a wide range of visible light from 348 nm (ultraviolet region), which means that the range of visible color change is wide due to the advantage of non-close packed colloidal crystal architecture.

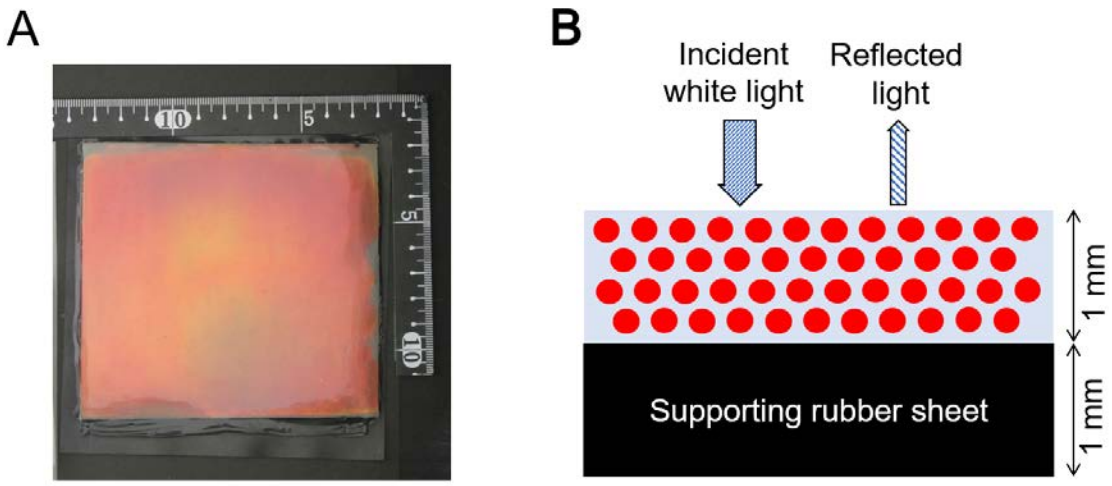

Figure 4. An elastic sheet of colloidal silica crystals arranged in a regular pattern in an elastomeric matrix. (**A**) Digital camera photograph of the surface of the sheet taken under coaxial illumination, showing the nearly red structural color spread over the entire area of the sheet. (**B**) Cross section of the rubber sheet and the concept of structural coloration by selective reflection. Incident white light is selectively reflected only in red by the colloidal crystal sheet. Light of other colors passes through the colloidal crystal layer and is absorbed in the black rubber sheet of the supporting substrate.

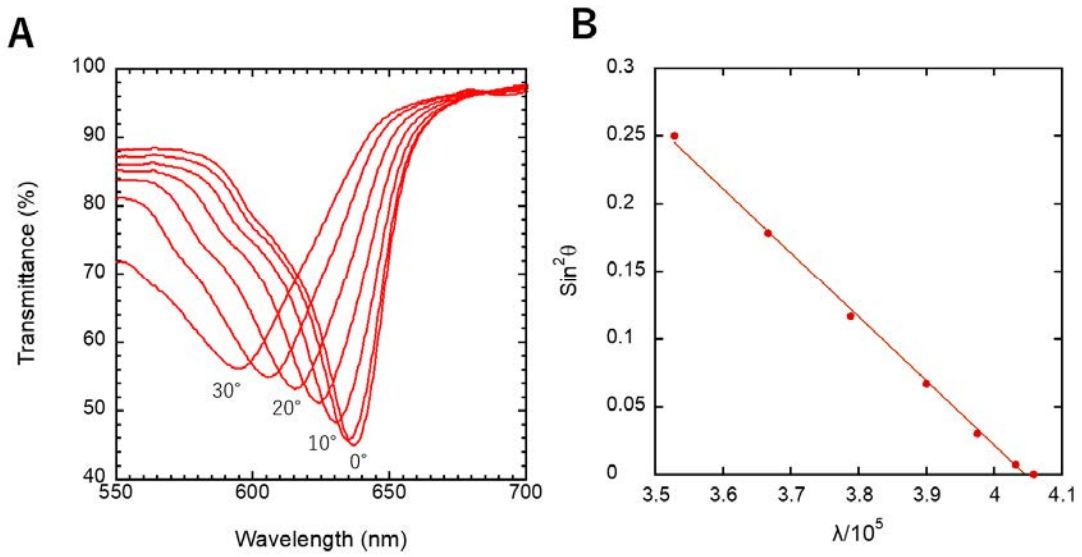

Figure 5. Measurement of the interplanar spacing of colloidal crystals in Poly(4-hydroxybutyl acrylate) using the Bragg-Snell formula. (**A**) Transmittance spectra measured at different angles, from 0° to 30° in 5° steps, (**B**) Measurement data plotted against wavelength and angle of incidence, showing a linear relationship between the two, and the interplanar spacing of the colloidal particles can be calculated from the angle of the straight line.

4.3. Mechnochromic of Silica Colloidal Crystal in Poly(4-HBA) Elastomer

Figure 6 shows the structural color change due to the application of basic mechanical forces; stretching, compressing, and bending. An initial red structural color shown in the photo A was changed to green color by horizontal directional stretching shown in the photo B. A disk-shaped sample sandwiched between two glass plates. The initial sample with no pressure shows a red structural color as shown in the photo C. On the other hand, the disk with pressure applied by the glass plate changed to green color as shown in the photo D. For bending deformation, there are two types, convex and concave, as shown in the photo E and the photo G. The original sheet shown in the photo F is red color. In the photo E, the structural color changed to green color by convex bending. In contrast in the photo G, the structural color changed to deep red color in the middle area by concave bending. The structural color change is available as a Supplementary Video S1.

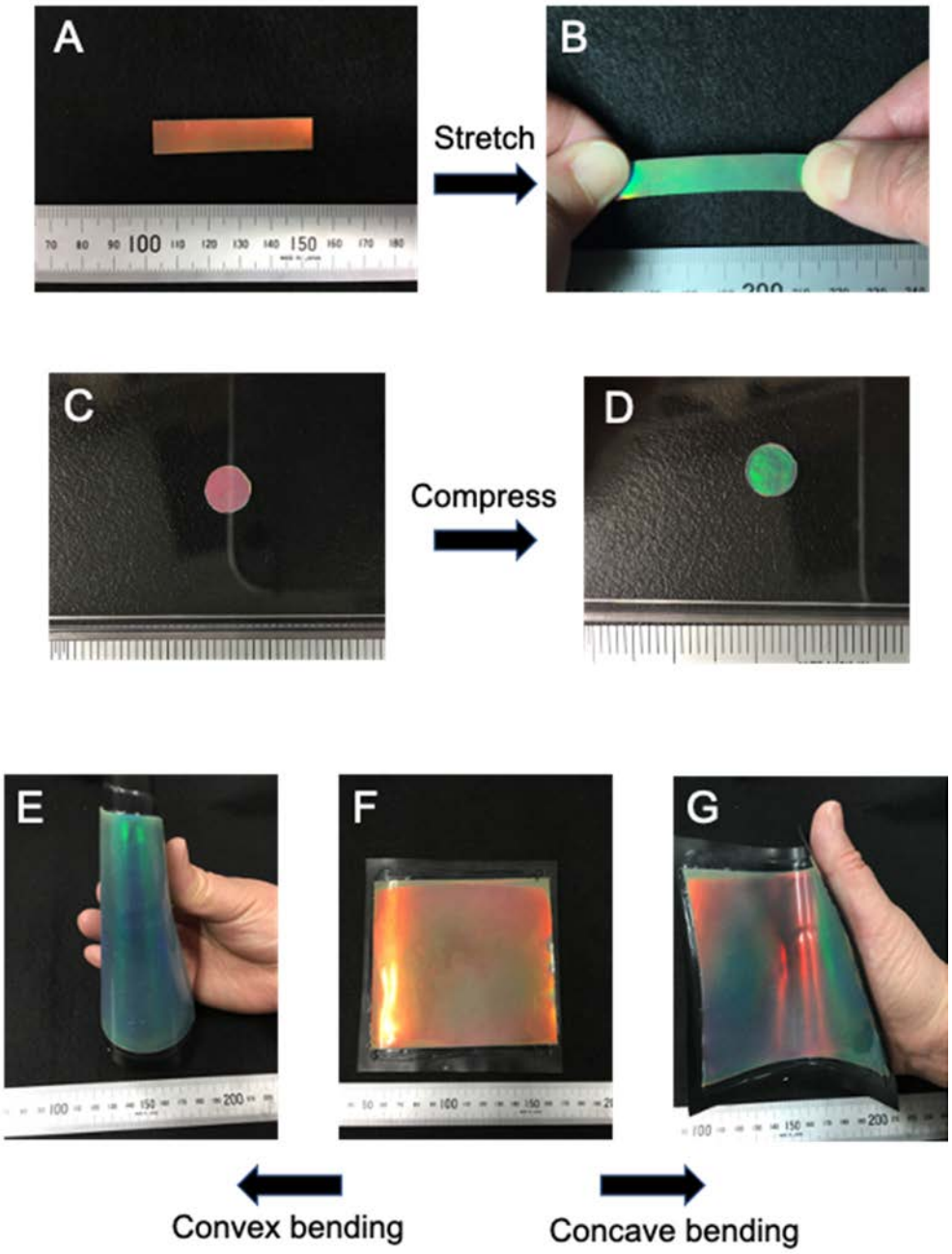

Figure 6. Structural color change due to mechanical-elastic different deformation modes. (**A**) an initial rectangular specimen, (**B**) under stretching, (**C**) an initial disk specimen, (**D**) under applied pressure by pressing a glass plate. (**E**–**G**) show the structural color change by convex and concave bending of a 100 mm square plate.

As the first deformation mode, the colloidal crystal was stretched in one direction using a single-axis stage. The change in structural color due to stretching is shown in the comparison images of coaxial irradiation in Supplementary Figure S4. Before stretching, the red structural color at 0 mm changes to green when stretched to 6 mm. When the stretching is stopped and the stage is returned to its initial state, the structural color returns perfectly to red. Structural color changes are quantitatively analyzed by Bragg diffraction analysis via reflection spectroscopy. Figure 7 show the elastic colloidal crystal was stretched to 8 mm in 1 mm increments and the reflectance spectrum was measured at each strain. Figure 7A shows that the Bragg's diffraction peak shifts to a lower wavelength direction and the reflection intensity decreases due to elongation. Figure 7B shows the relationship between the diffraction peak wavelength and elongation. When comparing the linear approximation and quadratic equation approximation on Figure 7B, the correlation coefficient R^2 is closer to 1 for the latter and expressed as following equation.

$$\lambda = 637.9 - 16.8\Delta L + 0.51\Delta L^2 \quad (2)$$

This result suggests that elastic colloidal crystal can be applied to tension sensor by elongation.

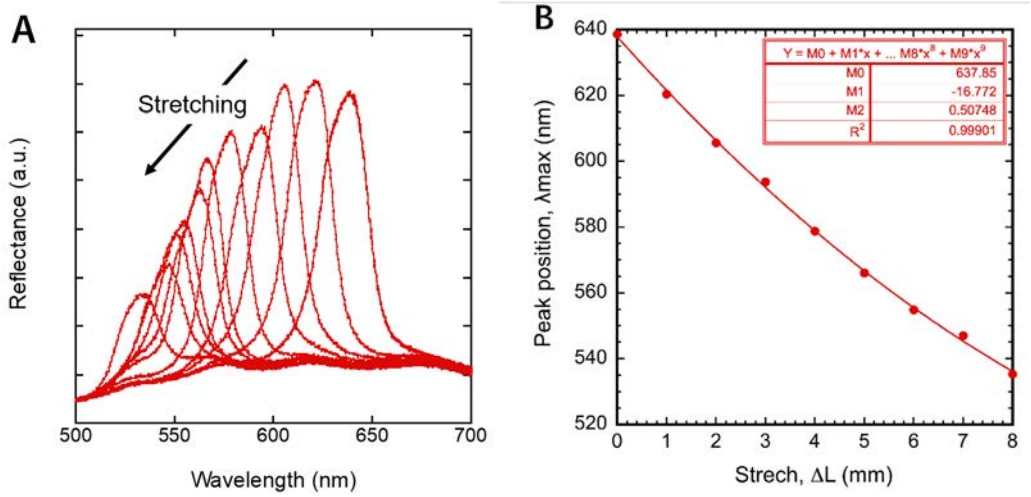

Figure 7. Analysis of structural color changes due to stretching using reflectance spectrometry. (**A**) Change in diffraction peak due to stretching, (**B**) relationship between peak wavelength and stretching length.

Next mechanical mode, we investigated structural color change by compressing deformation. A compression test on elastic colloidal crystals that had been punched out and molded into a disc shape using the equipment and setup described in Supplementary Figure S5. The concept idea of measurement is shown in illustration of Figure S5A. The sensing part of the probe is contacting to the surface of the top table of weigh meter photograph shown in the photo B. The diameter of the disk was 5.5 mm in diameter was mounted on the edge of probe shown in the photo C. The pressure applied to the disk sample came from compressing by vertical moving one dimensional precision stage and as measured by the weight meter. Figure 8 shows change of Bragg's diffraction peaks by increasing pressure on the disk. By increasing pressure, the Bragg diffraction peak shifted to a lower wavelength and its intensity also decreased monotonically (Figure 8A). The relationship between the peak wavelength and pressure is shown in Figure 8B. When comparing the correlation of the two-order approximation fit better than the first-order (linear). In this experiment, the increase in area due to compression was not taken into account. This should affect the approximation of the correlation, but it is currently difficult to measure, so we used the following equation.

$$\lambda = 624.2 - 2.1P + 0.024P^2 \quad (3)$$

By calibrating with the weight scale for each disk, the probe system of colloidal crystal elastomer can be used as a tactile sensor.

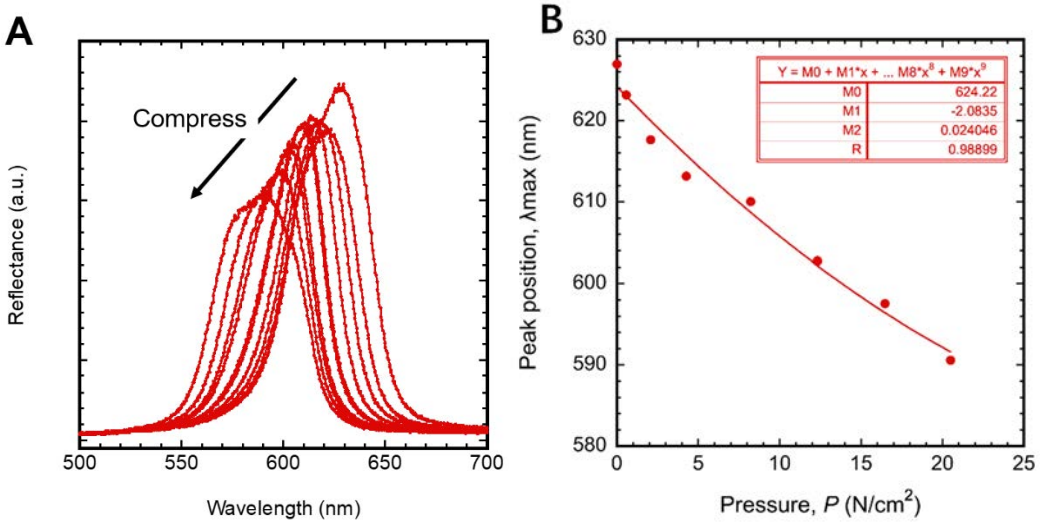

Figure 8. Analysis of structural color changes due to compression using reflectance spectrometry. (**A**) Change in diffraction peak due to compression, (**B**) relationship between peak wavelength and compression force.

Figure 9 shows a bending deformation mode. There are two types of bending, concave and convex, and they have different optical property. The concavity bending show in the photo A and the center indicates red color. In

contrast convexity bending show in the photo B and the center area indicates green color. To investigate the mechanical deformation on both bending, to compare Bragg's diffraction peak shifts shown in Figure 9D,E. In addition, the bending quantity was evaluated by deflection, d as shown in the photo C. As increasing deflection d, Bragg's diffraction peak shift to long wavelength in concavity bending. In contrast, Bragg's diffraction peak shift to short wavelength in convexity bending. The relationship deflection and peak position for both bending modes are shown in Figure 9F. A linear relationship is expressed as following equation.

$$\lambda = 616.4 - 28.28d \quad (4)$$

More detailed information on the mechanism of structural color changes in the two modes were investigated in Supplementary Figure S6. Photographs A, B, and C correspond to concave, flat, and convex curvature, respectively. The flat silica colloidal crystal elastomer shows a uniform red structural color for all area, and its cross-sectional view image is shown in Figure S6E. The elastic colloidal crystal sheet is composed of a 1 mm thick colloidal crystal sheet and a 1 mm thick black rubber sheet. The neutral axis of the bending deformation is the junction layer of the two parts. The plane spacing affects the compression and tension caused by bending. This is mainly the central region of the rubber sheet. In addition, the inclination angle of the plane also affects the structural color change caused by bending deformation. As shown in Figure S6D, the concave center part is subjected to compressive strain. As a result, the center part shows a deeply red color, and the two sides indicated by the white arrows show green and yellow. The color change on both sides is due to the sample tilting due to the concave bending deformation. As shown in Figure S6F, the convex central part is subjected to tensile strain. As a result, the colloidal crystal plane is compressed and the central part changes color to green. On the photo C, both side of the center area also may influence of tilting angle. However, it is not clear structural color change compare with the photo A. The phenomenon of peak shift due to bending deformation shift to longer or shorter wavelength has potential applications in bending sensors. However, bending deformation is dependent on the depth of the sample and produce tilting effect, it is complicated to be applied to sensor applications. Next, we investigated at the characteristics of long period stretching, and impacting phenomena as characteristics related to practical needs.

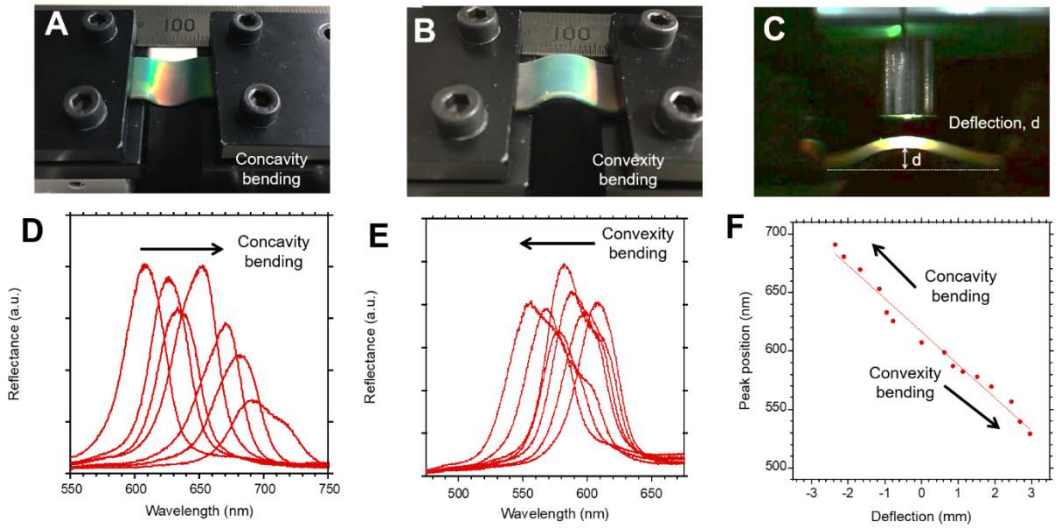

Figure 9. Analysis of structural color changes due to bending in convexity and concavity deformation. (**A**) concavity bending, (**B**) concvexity bending, (**C**) cross section image of the concvexity bending, (**D**) change in diffraction peak due to concavity bending, (**E**) change in diffraction peak due to concvexity bending and (**F**) a relationship deflection of bending and peak position.

4.4. Structural Color Material Properties for Practical Use

For structural color material properties for practical use, we will show two topics: Rapid structural color change by impaction and durability evaluation of repeatable elastic deformation. The former visualizes the change in the impact that the rubber sheet receives when a SUS steel ball falls as structural color. The video movies were shot in slow motion mode (240 frames per second, fps) using an iPhone camera. The details of the video shooting are shown in Supplementary Figure S7. An i-phone was set up below the position of the elastic colloidal crystal sheet. A steel ball was dropped and collided to the back rubber side and pressure was imaging bottom surface of the elastic colloidal crystal sheet. As a result, the structural color change enables to observe from downside. White LED backlighting (color temperature 5000 K) was applied to white diffused glass at an angle of approximately

45 degrees, and the reflected light was applied to the rubber sheet from below side. The pressure distribution image on the rubber sheet was acquired by the camera of the i-phone through the transparent acrylic plate. Figure S7B shows a series of each snap shot images at 240 fps mode. One frame (f) is equivalent to 1/240 of a second, or 0.004167 s. This is equivalent to 4.17 milliseconds. This means the 10th frame image is after 37.6 ms from the 1st frame. We can obtain high speed camera images with 4.17 ms resolution. The video movie can be available in Supplementary Video S2. Another movie was analyzed as shown in Figure 10. The position of the impact was first confirmed in the second frame. In the fifth frame, the color changes to a vivid green. In the seventh frame, the structural color of the second position changes due to the second collision of the rebounding steel ball. In the twentieth frame, the third position changes color. The structural color change caused by compression due to the collision can be visualized as a high-speed phenomenon with a minimum step of 4.17 ms or less. On the other hand, it takes some time for the elastically deformed area to return to its original shape, and the structural color change (from green to red) is slower than the collision. However, it recovered to its original structural color of red within one second. From these results, it is expected that by using a high-resolution high-speed camera, it will be possible to visualize collision phenomena of less than 1 mS as structural color changes, and by using the correlation with compression phenomena shown in Figure 8, it will be possible to analyze the change in stress distribution at high speeds. In this experiment, the slow-motion function of a commercially available general-purpose smartphone was utilized. The employment of a high-resolution high-speed camera will facilitate the capture of high-speed phenomena with enhanced precision, which is anticipated to be instrumental in elucidating collision phenomena.

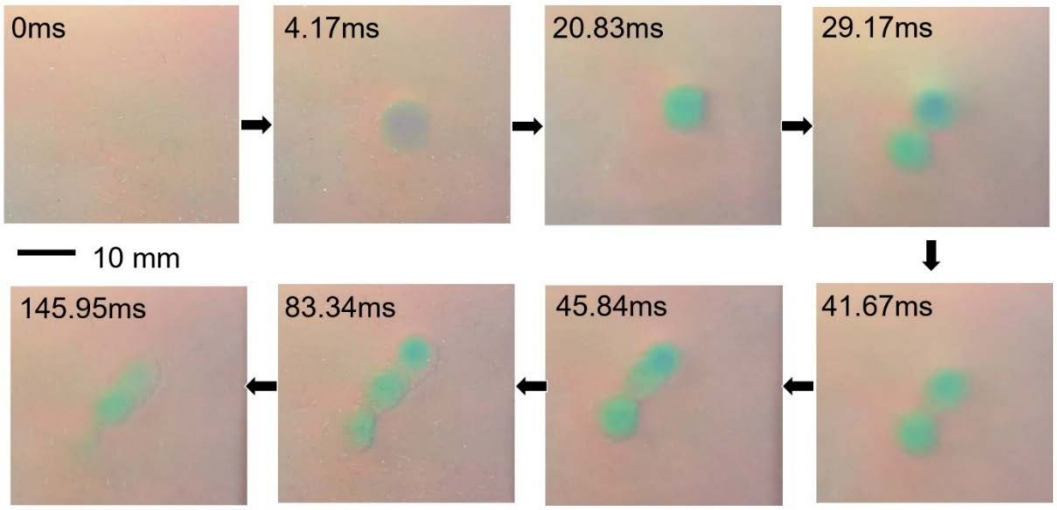

Figure 10. Rapid structural color change by impacting on a steal ball on an elastic colloidal crystal sheet shown in Figure 3A. The images were taken by 240 frames per second (fps) movie mode of iPhone camera. Eight snapshots corresponding to 0 ms to 145.95 ms, respectively.

One of issues on strain sensor issues to be addressed for practical application is the evaluation of durability against repeated elastic deformation. The desktop device (DMLHP-PP, Yuasa System Co., Ltd.) used in the evaluation test is shown in Figure S8. The photo A shows the appearance of the device. The rubber sheet was stretched in one direction by 15 mm at a rate of 15 times per minute (The video movie can be available in Supplementary Video S3). The photo B is a snapshot of the state before stretching, and the photo C is a snapshot of the state after stretching. The former shows a red structural color, and the latter shows a green structural color. As a durability test, we decided to check whether the structural color change function of the elastic colloidal crystal could be maintained after 10,000 or 100,000 cycles of stretching. The evaluation results are shown in Figure 11. The graph A shows the reflectance spectrum of the rubber sheet with initial state (sample length of 40 mm) and stretching (sample length of 50 mm) before durability test. The red line shows the structural color of initial state with a peak wavelength 600.0 nm. In contrast, stretched 10 mm from its unloaded state shows green structural color with a peak wavelength 560.5 nm. Figure 11B shows comparison three state conditions. It was confirmed that the structural color changes with elastic deformation and that this function is maintained even after 100,000 cycle tests. There is no change or damage after durability test. Although there is a little variation in the peak wavelength due to differences in the measurement points, we can conclude that the durability of the material is not a problem.

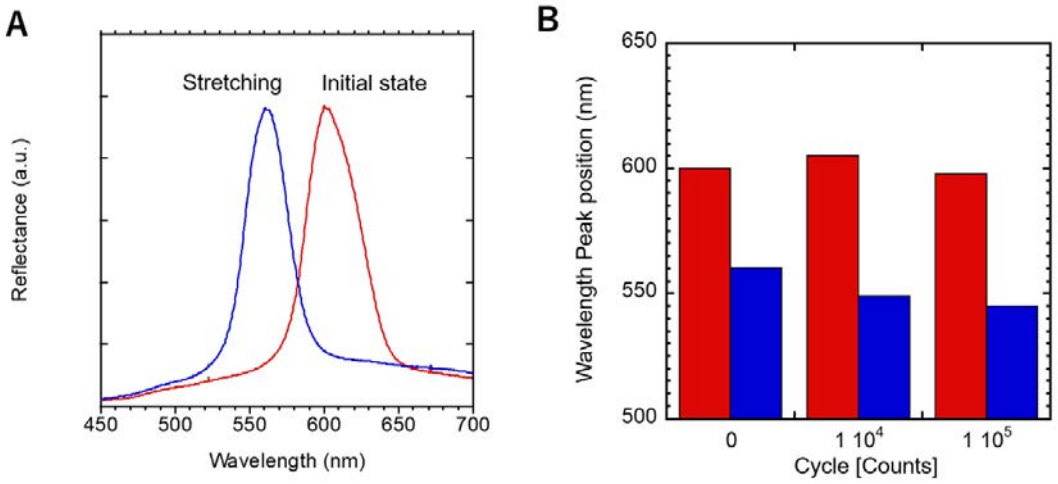

Figure 11. Evaluation of durability by repeated stretching. (**A**) comparing the initial state (length of sample: 40 mm) and after stretched (50 mm), (**B**) Comparison of peak wavelengths after repeated stretching of the sample. Red bar (no stretching) and blue bar (under stretched) after 0, 10,000 and 100,000 cycles elastic deformation.

5. Conclusions

By embedding non-close packed colloidal crystals of silica colloidal particles in polyacrylate elastomer, we fabricate smart material sheet whose structural color changes with elastic deformation.

The formation of this colloidal crystal elasticity was achieved by aligning the silica particle orientation planes through desalination and shear stress using ion exchange resin. In addition, the monomer 4-HBA was polymerized through UV irradiation radical polymerization. The lattice constant of the initial colloidal crystal depended on the particle concentration, and by adjusting it to 20 wt%, the structural color of the colloidal crystal was designed to be red. This elastic sheet was made from 1 mm thick 4-HBA polyacrylate with 150 nm silica particles oriented in one direction at distance of 225 nm between the surfaces. By attaching it to a 1 mm thick black rubber sheet, it becomes a rubber sheet that reversibly changes color with deformation, with a vivid structural color.

In this paper, we investigated three basic mechanical deformation modes (stretching, compression, and bending) as well as impact and durability. In stretching and compression, the peak wavelength of the Bragg diffraction that causes structural color was found to be simple correlated with the amount of stretching, compression stress, and bending (displacement). On bending is two type mode of deformation, concavity and convexity. On concavity bending deformation, peak shift to shorter wavelength. In contrast, concavity deformation, the peak shift to longer wavelength. Bending is also corresponding a simple relationship between peak position and deflection. These three modes suggest that mechanical deformation is applied to smart sensing. In finally, using a high-speed camera, rapid strain changes images on 5 ms order were obtained in the impacting test. The imaging function the strain mapping enables wide applications from sport to industry. Finally, the durability test for elongation suggests that practically application use. 100,000 cycle stretching the rubber has kept the tunable structural color function.

Supplementary Materials: The supporting information can be downloaded at: https://media.sciltp.com/articles/others/250151015568327/MI-Supplement.zip.

Author Contributions: T.S.: conceptualization, methodology, preparation writing—reviewing and editing; H.F.: data curation, writing—original draft; S.K.: Synthesis silica and prepolymer suspension, investigation; F.U.: Synthesis silica and prepolymer suspension, its supervision. All authors have read and agreed to the published version of the manuscript.

Funding: This research was funded by JSPS KAKENHI Grant Number JP2135017.

Data Availability Statement: The data presented in this study are available upon request from the corresponding author.

Acknowledgments: We thank for Chikako Tsuda and Kaori Terui for their experimental works. Chikako measured photonic functional property and photo pictures. Kaori prepared silica suspensions dispersed in 4-HBA monomer liquid.

Conflicts of Interest: The authors declare no conflict of interest.

References

1. Clough, J.M.; Weder, C.; Schrettl, S. Mechanochromism in structurally colored polymeric materials. *Macromol. Rapid Commun.* **2021**, *42*, 2000528.
2. Xie, M.; Hisano, K.; Zhu, M.; Toyoshi, T.; Pan, M.; Okada, S.; Tsutsumi, O.; Kawamura, S.; Bowen, C. Flexible multifunctional sensors for wearable and robotic applications, *Adv. Mater. Techn.* **2019**, *4*, 1800626.
3. Sandt, J.D.; Moudio, M.; Clark, J.K.; Hardin, J.; Argenti, C.; Carty, M.; Lewis, J.A.; Kolle, M. Stretchable optomechanical fiber sensors for pressure determination in compressive medical textiles, *Adv. Healthcare Mater*. **2018**, *7*, 1800293.
4. Kolle, M.; Zheng, B.; Gibbons, N.; Baumberg, J.J.; Steiner, U. Stretch-tuneable dielectric mirrors and optical microcavities. *Opt. Express* **2010**, *18*, 4356–4364.
5. Chan, E.P.; Walish, J.J.; Thomas, E.L.; Stafford, C.M. Block copolymer photonic gel for mechanochromic sensing, *Adv. Mater.* **2011**, *23*, 4702–4706.
6. Park, T.H.; Yu, S.; Cho, S.H.; Kang, H.S.; Kim, Y.; Kim, M.J.; Eoh, H.; Park, C.; Jeong, B.; Lee, S.W.; et al. Block copolymer structural color strain sensor. *NPG Asia Mater.* **2018**, *10*, 328–339.
7. de Castro, L.D.C.; Engels, T.A.P.; Oliveira, O.N., Jr.; Schenning, A.P.H.J. Sticky multicolor mechanochromic labels. *ACS Appl. Mater. Interfaces* **2024**, *16*, 11, 14144–14151.
8. Li, M.; Lyu, Q.; Peng, B.; Chen, X.; Zhang, L.; Zhu, J. Bioinspired colloidal photonic composites: Fabrications and emerging applications. *Adv. Mater.* **2022**, *34*, 2110488.
9. Fudouzi, H.; Sawada, T.; Photonic rubber sheets with tunable color by elastic deformation. *Langmuir* **2006**, *22*, 1365–1368.
10. Arsenault, A.C.; Clark, T.J.; von Freymann, G.; Cademartiri, L.; Sapienza, R.; Bertolotti, J.; Vekris, E.; Wong, S.; Kitaev, V.; Manners, I.; et al. From colour fingerprinting to the control of photoluminescence in elastic photonic crystals. *Nat. Mater.* **2006**, *5*, 179–184.
11. Finlayson, C.E.; Goddard, C.; Papachristodoulou, E.; Snoswell, D.R.E.; Kontogeorgos, A.; Spahn, P.; Hellmann, G.P.; Hess, O.; Baumberg, J.J. Ordering in stretch-tunable polymeric opal fibers. *Opt. Express* **2011**, *19*, 3144–3154.
12. Liang, H.L.; Bay, M.M.; Vadrucci, R.; Barty-King, C.H.; Peng, J.; Baumberg, J.J.; De Volder, M. F. L.; Vignolini, S.; Roll-to-roll fabrication of touch-responsive cellulose photonic laminates. *Nat. Commun*. **2018**, *9*, 4632.
13. Zhao, Q.; Finlayson, C.; Snoswell, D.; Haines, A.; Schäfer, C.; Spahn, P.; Hellmann, G.P.; Petukhov, A.V.; Herrmann, L.; Burdet, P.; et al. Large-scale ordering of nanoparticles using viscoelastic shear processing. *Nat. Commun.* **2016**, *7*, 11661.
14. Kamenetzky, E.A.; Magliocco, L.G.; Panzer, H.P.; Structure of solidified colloidal array laser filters studied by cryogenic transmission electron microscopy. *Science* **1994**, *263*, 207–210.
15. Lee, G.H.; Choi, T.M.; Kim, B.; Han, S.H.; Lee, J.M.; Kim, S.-H. Chameleon-inspired mechanochromic photonic films composed of non-close-packed colloidal arrays. *ACS Nano* **2017**, *11*, 11350–11357.
16. Miwa, E.; Watanabe, K.; Asai, F.; Seki, T.; Urayama, K.; Odent, J.; Raquez, J.M.; Takeoka, Y.; Composite elastomer exhibiting a stress-dependent color change and high toughness prepared by self-assembly of silica particles in a polymer network. *ACS Appl. Polym. Mater.* **2020**, *2*, 4078.
17. Inci, E.; Topcu, G.; Demir, M.M. Colloidal films of SiO_2 in elastomeric polyacrylates by photopolymerization: A strain sensor application. *Sens. Actuators B* **2020**, *305*, 127452.
18. Kanai, T.; Sawada, T.; Toyotama, A.; Kitamura, K. Air-pulse-drive fabrication of photonic crystal films of colloids with high spectral quality. *Adv. Funct. Mater.* **2005**, *15*, 25–29.
19. Tajima, H.; Amano, A.; Kanai, T. Elastomer-immobilized tunable colloidal photonic crystal films with high optical qualities and high maximum strain. *Mater. Adv.* **2021**, *2*, 3294–3299.
20. An, T.; Jiang, X.; Gao, F.; Schäfer, C.; Qiu, J.; Shi, N.; Song, X.; Zhang, M.; Finlayson, C.E.; Zheng, X.; et al. Strain to shine: Stretching-induced three-dimensional symmetries in nanoparticle-assembled photonic crystals. *Nat. Commun.* **2024**, *15*, 5215.
21. Miyake, D.; He, J.; Asai, F.; Hara, M.; Seki, T.; Nishimura, S.; Tanaka, M.; Takeoka, Y. Optically Transparent and Color-Stable Elastomer with Structural Coloration under Elongation. *Langmuir* **2023**, *39*, 17844–17852.
22. Peng, L.; Hou, L.; Wu, P. Synergetic Lithium and Hydrogen Bonds Endow Liquid-Free Photonic Ionic Elastomer with Mechanical Robustness and Electrical/Optical Dual-Output. *Adv. Mater.* **2023**, *35*, 2211342.
23. Li, X.; Cheng, Y.; Zhou, Y.; Shi, L.; Sun, J.; Ho, G.W.; Wang, R. Programmable Robotic Shape Shifting and Color Morphing Dynamics Through Magneto-Mechano-Chromic Coupling. *Adv. Mater.* **2024**, *36*, 2406714.
24. Fudouzi, H.; Sawada, T. Colloidal photonic crystals made of soft materials: Gels and elastomers. In *Micro and Nanophotonic Technologies*, 1st ed.; Meyrueis, P., Van de Voorde, P.M., Sakoda, K., Eds.; Wiley-VCH: Weinheim, Germany, 2017; pp. 507–526.
25. Ackerson, B.J.; Pusey, P.N. Shear-induced order in suspensions of hard spheres. *Phys. Rev. Lett*. **1988**, *61*, 1033.

26. Kawanaka, S.; Uchida, F.; Sawada, T.; Furumi, S.; Fudoji, H. *Sheet of Colloidal Crystals Immobilized in Resin, Method for Displaying Structural Color Using Same, Method for Detecting Unevenness Distribution or Hardness Distribution of Subject Using Same, and Structural Color Sheet*; International Application Publication: Tokyo, Japan, 2015; 86p.
27. Fudouzi, H. Fabricating high-quality opal films with uniform structure over a large area. *J. Colloid. Interface Sci.* **2004**, *275*, 277–283.